scientific reports

Check for updates

OPEN

Artificial intelligence-based prediction of radio-cephalic arteriovenous fistula maturation using preoperative duplex examination: a retrospective multicenter cohort study

Ara Cho[1,6], Sanghyun Ahn[1,6], Jang Yong Kim[2], JungKyun Hyun[3], YongHwan Kim[5] & Hyangkyoung Kim[4]✉

Establishing a functional arteriovenous fistula (AVF) is crucial to ensure effective dialysis treatment. However, there are currently no definitive criteria for predicting AVF maturation using preoperative ultrasound. This study aims to assess the efficacy of AI-driven models in analyzing comprehensive ultrasonographic variables across multiple forearm locations to predict successful AVF maturation. A retrospective analysis was conducted on 492 cases within a cohort of 494 individuals who underwent radiocephalic arteriovenous fistula (AVF) creation across three centers over a span of four years. The analysis involved various variables such as demographic data, cephalic vein diameters at distal (vein 1), mid (vein 2), and proximal (vein 3) locations, vein wall thickness, competing tributaries, peak systolic velocity, and radial artery waveform. To assess the predictive value of these variables, XGBoost, a machine learning model, was utilized. Significant predictors of AVF maturation included cephalic vein diameters (distal, mid, and proximal) with p-values of 0.004, 0.003, and 0.009, respectively, and competing tributaries ($p < 0.001$). The optimal model performance was in Stage 4, excluding vein 1 data, achieving an F1 score of 0.883, a Matthews Correlation Coefficient of 0.741, and an AUC of 86.9%. A vein 2 diameter cut-off of 4.5 mm resulted in an 89.5% success rate in maturation. This study underscores the value of comprehensive ultrasonographic assessments in predicting AVF maturation, advocating for detailed preoperative ultrasound mapping of the entire forearm to enhance AVF outcomes.

A well-functioning arteriovenous fistula is essential for high-quality dialysis, as it reduces morbidity, prolongs patient survival, and enhances quality of life. Autologous arteriovenous fistulas (AVF) are the preferred choice for vascular access due to their superior performance compared to grafts and hemodialysis catheters in terms of long-term usage, infection rates, and mortality[1]. The National Kidney Foundation Kidney Disease Outcomes Quality Initiative (NKF-KDOQI) Guideline and the National Vascular Access Improvement Initiative advocated for radiocephalic arteriovenous fistula (RCAVF) as the primary option for vascular access, where feasible. Traditionally, routine preoperative ultrasound mapping for AVF construction was considered essential for successful fistula development[2,3]. However, recent NKF-KDOQI guidelines have challenged the necessity of routine preoperative ultrasound mapping, citing a lack of supporting evidence[4]. Instead, selective mapping was recommended for patients at high risk of fistula failure, such as the elderly, females, those with comorbidities, and small pediatric patients.

[1]Department of Surgery, Seoul National University hospital, Seoul, Korea. [2]Departments of Surgery, The Catholic University of Korea, St. Mary's Hospital, Seoul, Korea. [3]Department of Healthcare and Artificial Intelligence, Catholic University of Korea, Seoul, Korea. [4]Department of Surgery, Ewha Womans University College of Medicine, Ewha Womans University Medical Center, 07985, 1071, Anyangcheon-ro, Yangcheon-gu, Seoul, Korea. [5] Spass Incorporation, Seoul, Korea. [6]Ara Cho and Sanghyun Ahn contributed equally to this work. ✉email: hkkim77@ewha.ac.kr

Chronic kidney disease (CKD) patients commonly present with comorbidities such as hypertension, diabetes, and cardiovascular disease. A large-scale prevalence study indicated that 98.2% of adults with CKD had at least one comorbidity[5]. This often leads to frequent hospitalizations that require multiple venipunctures, indicating that most CKD patients are at high risk[6]. As a result, relying solely on physical ex-amination may not provide a complete assessment of cephalic vein quality in these patients. This limitation emphasizes the significance of alternative diagnostic tools. However, there have been conflicting reports regarding the predictive value of pre-operative ultrasound mapping[7–11]. We hypothesized that the disparities in these results might result from the analysis being based on insufficient information about the preoperative condition. Therefore, this study aimed to evaluate the predictive values of variables including ultrasonographic findings and demographic information using AI modeling for successful fistula development.

Results

A total of 492 eligible cases were included in the analysis. Of the 492 eligible cases analyzed, 135 cases (27.4%) experienced maturation failure, resulting in an overall maturation rate of 72.6%. Demographic data, ultrasound variables, and study outcomes are summarized in Table 1. None of the cases in this cohort had maturation failure due to the need for superficialization of the cephalic vein caused by access depth. In the initial statistical analysis, all diameters of the fore-arm cephalic veins were found to be significantly associated with maturation status ($p = 0.004$, $p = 0.003$, and $p = 0.009$ for vein 1, vein 2, and vein 3, respectively). Among the 75 patients (15.3%), vein 1 had a diameter smaller than 2 mm. This condition was correlated with 35 cases (25.9%) of maturation failure, showing a statistically significant association ($p < 0.001$). The presence of a competing tributary was also significantly associated with maturation failure ($\chi 2 = 13.63$, $p < 0.001$).

Model performance

The results of the model performance are presented in Table 2; Fig. 1. Among the variables used in Stage 1, vein 1 made a more significant contribution to the prediction performance compared to sex or age (Fig. 1A). The overall performance of Stage 1 was inferior to that of the other stages (F1 = 0.624 and MCC= −0.061 with Neural Network). Moving on to Stage 2, the model exhibited higher performance compared to the previous stage (F1 = 0.773, MCC = 0.397 using a Neural Network). The overall model performance in Stage 4, where vein 1 was excluded from Stage 2, showed superior performance compared to all other stages (F1 = 0.869, MCC = 0.624 using XGBoost). In Stage 5, the model included all variables from Stage 4 except for vein wall thickness. The best model performance in Stage 5 was achieved using the Neural Network, showing slightly worse performance compared to Stage 4 (F1 = 0.726, MCC = 0.298 using XGBoost). The significance of vein 2 was apparent across most modeling procedures, along with vein 3, whereas other ultrasonographic features such as PSV or the waveform of the radial artery were relatively less important (Fig. 1).

Final prediction model

The XGBoost model for Stage 4 was found to be the optimal prediction model due to its superior performance, as shown in Fig. 2. The Area Under the Curve was 87.3% for Stage 4 (Fig. 2B), compared to 53.4% for Stage 1 (Fig. 2A), indicating better prediction of Stage 4 model. When comparing the calibration slope, the slope for Stage 4 was generally closer to 1, indicating that the model's predictions are well calibrated to the observed probabilities (Fig. 3). In particular, it was determined that setting the cut-off value of vein 2 at 4.5 mm would achieve an 89.5% success rate in maturation.

	All eligible participants ($n = 492$)	Maturation success ($n = 357$)	Maturation failure ($n = 135$)	p-value
Age	63 (52–72)	63 (52–72)	62 (55–72.5)	0.980
Sex (men)	315 (64.2)	233 (65.4)	82 (60.7)	0.344
Diameter (mm)				
Vein 1 (distal)	2.6 (2.1–3.1)	2.7 (2.2–3.1)	2.4 (1.9–2.9)	0.001
Vein 2 (mid)	3.0 (2.4–3.5)	3.1 (2.6–3.6)	2.4 (1.8–3.1)	< 0.001
Vein 3 (proximal)	3.4 (2.8–4.2)	3.6 (3.0–4.3)	3.0 (2.1–3.7)	< 0.001
Artery	2.25 (2–2.5)	2.3 (2.0–2.5)	2.2 (2.0–2.5)	0.358
Vein wall thickness (mm)	0.080 (0.056–0.128)	0.063 (0.052–0.102)	0.105 (0.077–0.154)	< 0.001
Tributary*	44 (9.0)	21 (5.9)	23 (17.0)	< 0.001
PSV (cm/s)	50.1 (29.0–68.4)	47.5 (21.2–69.3)	51.2 (36.6–64.5)	0.238
Arterial waveform				0.472
Biphasic	42 (8.6)	28 (66.7)	14 (33.3)	
triphasic	344 (70.1)	248 (72.1)	96 (27.9)	

Table 1. Patients' characteristics and study outcome. IQR, interquartile range; PSV, peak systolic velocity. All values are presented as the median (interquartile range) for continuous variables or as n (%) for categorical variables. *Presence of tributary of similar diameter.

	AUC	F1	Precision	Recall	MCC	Specificity
Stage 1						
Gradient Boosting (XGBoost)	**0.412**	0.613	0.591	0.646	−0.059	0.305
Logistic Regression	0.408	0.629	0.547	0.740	0.000	0.260
Naïve Bayes	0.373	0.617	0.577	0.688	−0.075	0.268
Neural Network	0.337	0.624	0.545	0.729	−0.061	0.257
Random Forest	0.409	0.613	0.591	0.646	−0.059	0.305
Stage 2						
Gradient Boosting (XGBoost)	0.604	0.719	0.713	0.740	0.244	0.468
Logistic Regression	0.712	0.752	0.764	0.781	0.350	0.482
Naïve Bayes	**0.717**	0.743	0.738	0.750	0.318	0.549
Neural Network	0.652	0.773	0.769	0.781	0.397	0.586
Random Forest	0.634	0.725	0.722	0.729	0.279	0.542
Stage 3						
Gradient Boosting (XGBoost)	0.799	0.781	0.777	0.789	0.401	0.579
Logistic Regression	**0.878**	0.854	0.853	0.855	0.608	0.741
Naïve Bayes	0.849	0.868	0.868	0.868	0.649	0.781
Neural Network	0.850	0.801	0.799	0.803	0.465	0.654
Random Forest	0.806	0.801	0.799	0.803	0.465	0.654
Stage 4						
Gradient Boosting (XGBoost)	0.833	**0.869**	0.884	0.885	**0.624**	0.834
Logistic Regression	**0.869**	0.727	0.725	0.731	0.391	0.648
Naïve Bayes	0.833	0.810	0.814	0.808	0.588	0.794
Neural Network	0.797	0.805	0.804	0.808	0.566	0.741
Random Forest	0.853	0.841	0.847	0.846	0.652	0.762
Stage 5						
Gradient Boosting (XGBoost)	**0.673**	0.630	0.619	0.646	0.034	0.385
Logistic Regression	0.567	0.645	0.632	0.667	0.068	0.393
Naïve Bayes	0.741	0.697	0.711	0.688	0.265	0.594
Neural Network	0.602	0.726	0.723	0.729	0.298	0.561
Random Forest	0.621	0.601	0.584	0.625	−0.053	0.329

Table 2. The model performance in each stage. AUC, area under the receiver operating characteristic curve; MCC, Matthews Correlation Coefficient.

Discussion

Historically, routine preoperative ultrasound mapping was seen as necessary for creating an AVF[2]. The purpose was to find suitable veins for cannulation, understand their anatomy, and anticipate any potential obstacles that could hinder the successful maturation of the AVF. However, recent guidelines, including the NKF-KDOQI guidelines, have changed their view on the obligatory use of routine preoperative mapping. They argue that there is insufficient high-quality evidence to support its routine application[4]. By advocating for selective ultrasound mapping in high-risk patients, such as the elderly, females, and those with comorbidities, the updated guidelines aim to optimize resource utilization and improve clinical outcomes, while ensuring successful AVF creation. This shift reflects insufficient supporting evidence of its value in im-proving primary patency or preventing maturation failure[3]. Additionally, the potential drawbacks of routine mappings, such as increased procedure time and cost, have gained greater consideration[4]. Therefore, selective mapping is now recommended. However, the dialysis population has increased in age and accumulated more comorbidities, both of which are regarded as high risks for AVF failure[12]. Logically, many preoperative patients fall into this high-risk category. Even in patients with a lower risk, a physical examination often fails to provide information on the entire length of the vessel. This justifies routine mapping as a matter of common sense. However, currently, the role of preoperative ultrasound mapping remains unclear due to conflicting reports on its predictive value regarding AVF maturation[10,11]. This discrepancy may arise from two main factors: either the ultrasound variable included in the studies differed, or there was inconsistency in the diagnostic criteria or examination protocol. Typically, ultrasound diagnostic criteria use a venous diameter cutoff value of 2 mm at the anastomotic sites. In terms of outcomes, preoperative mapping was evaluated by either the maturation failure rate or the patency rate. In this study, we aimed to determine which variables should be included in preoperative ultrasonographic mapping. We specifically focused on maturation failure as the outcome variable and limited the study to RCAVFs to ensure homogeneity of results. Our investigation revealed that the specificity for predicting maturation when the preoperative evaluation was based solely on wrist cephalic vein diameter, age, and sex was only 30.5%. This highlights the need for additional evaluation tools to assist in preoperative planning.

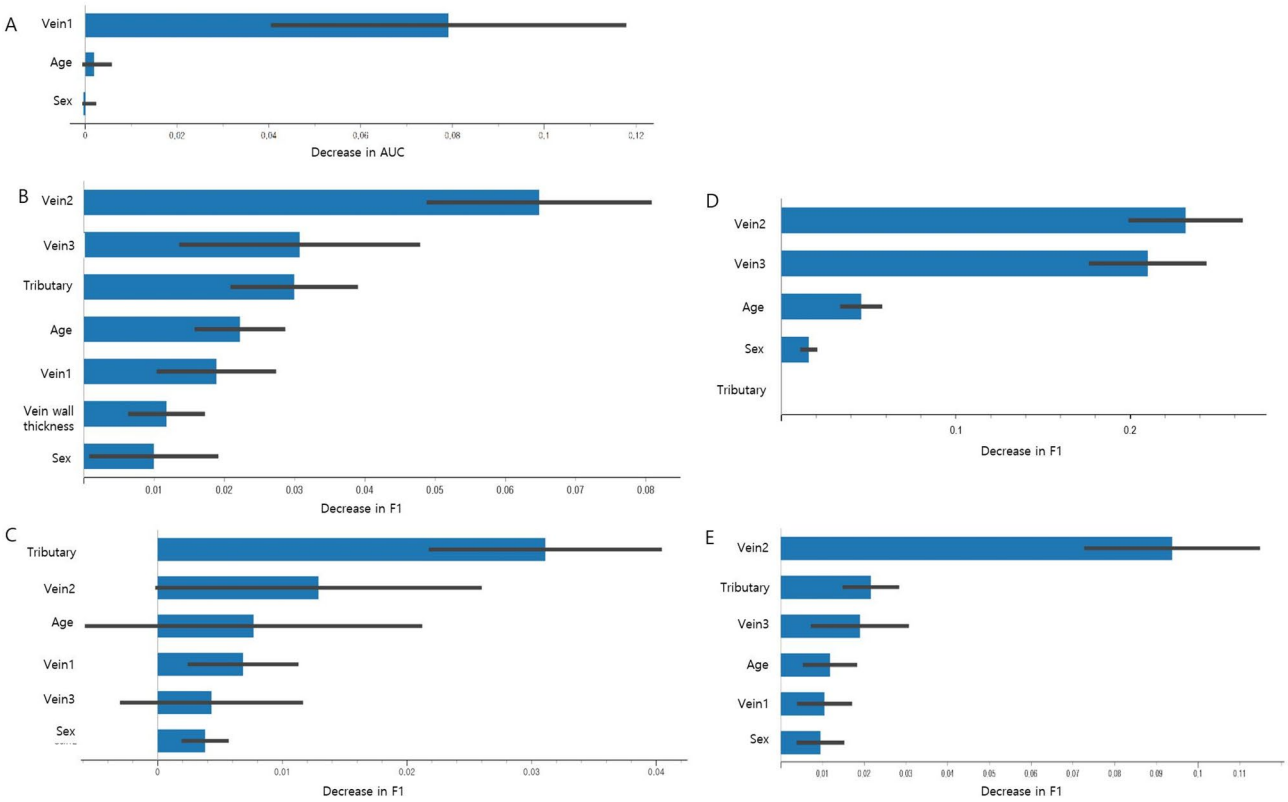


Fig. 1. Model performance of each stage. (**A**) Stage 1, (**B**) Stage 2, (**C**) Stage 3, (**D**) Stage 4, (**E**) Stage 5. Vein 1 demonstrated more significant contribution to the prediction performance compared to other factors in stage 1. Stage 2 model exhibited higher performance than stage 1. The stage 4 exhibited greater performance than other stages.

There is variability in AVF maturation criteria reported globally. The rule of 6 (flow volume > 600mL/min, vein diameter > 6 mm, vein depth < 6 mm) is widely used to determine when to start hemodialysis[13,14]. Others recommend vein diameter above 4 mm and volume flow above 500mL/min as successful maturation criteria[15]. To address this, we used definitions based on successful maturation with the ease of cannulation, the ability to have three consecutive sessions of hemodialysis for at least four hours, and a blood flow rate of 250 mL/min or more. Any thrombosis or unable to puncture the vein or finish hemodialysis was defined as maturation failure.

In our study, mid- and proximal-forearm cephalic vein diameter, age, and sex emerged as important variables to consider, particularly from stage 4, exhibiting superior performance with an 86.9% AUC. Our model's strong performance from stage 4 suggests that these variables play a crucial role during this phase, highlighting the importance of detailed vascular assessment in predictive modeling for RCAVF maturation. It's important to note that distal forearm diameters were often similar to or larger than 2 mm in most cases. Consequently, many cases were selected either through preoperative mapping or direct visual evaluation intraoperatively, as suggested in previous literature[16–19]. This selection bias may have led to an underestimation of the distal forearm cephalic vein diameter's significance in the model's predictive performance. To provide context for our findings, Table 3 summarizes recent state-of-the-art models for AVF maturation prediction. The table compares datasets, features used, predictive performances, and key methodological differences[20,21]. Our XGBoost-based model demonstrates competitive or superior performance compared to previous approaches, benefiting from detailed ultrasonographic features and clinical variables. Thus, it is recommended that, during the preoperative mapping procedure, measurements of all forearm cephalic vein diameters—representing distal, mid, and proximal forearm sites—should be considered when constructing a RCAVF. Furthermore, the presence of competing tributaries was found to be significantly associated with maturation failure in descriptive analytics and remained important in most stages, except stage 4.

There are several limitations to acknowledge in our study. Firstly, it was conducted retrospectively, which inherently limits control over variables. This study focused on ultrasound-derived parameters and did not incorporate additional clinical variables, such as diabetes mellitus, prior puncture history, or dialysis vintage. These factors are known to influence vascular condition and may affect arteriovenous fistula maturation. However, such underlying changes are likely reflected in morphologic and hemodynamic features observed on duplex ultrasound. Therefore, this study aimed to evaluate whether imaging alone could provide sufficient predictive information without detailed clinical history. Nevertheless, incorporating both imaging and clinical variables may further improve predictive performance in future models.

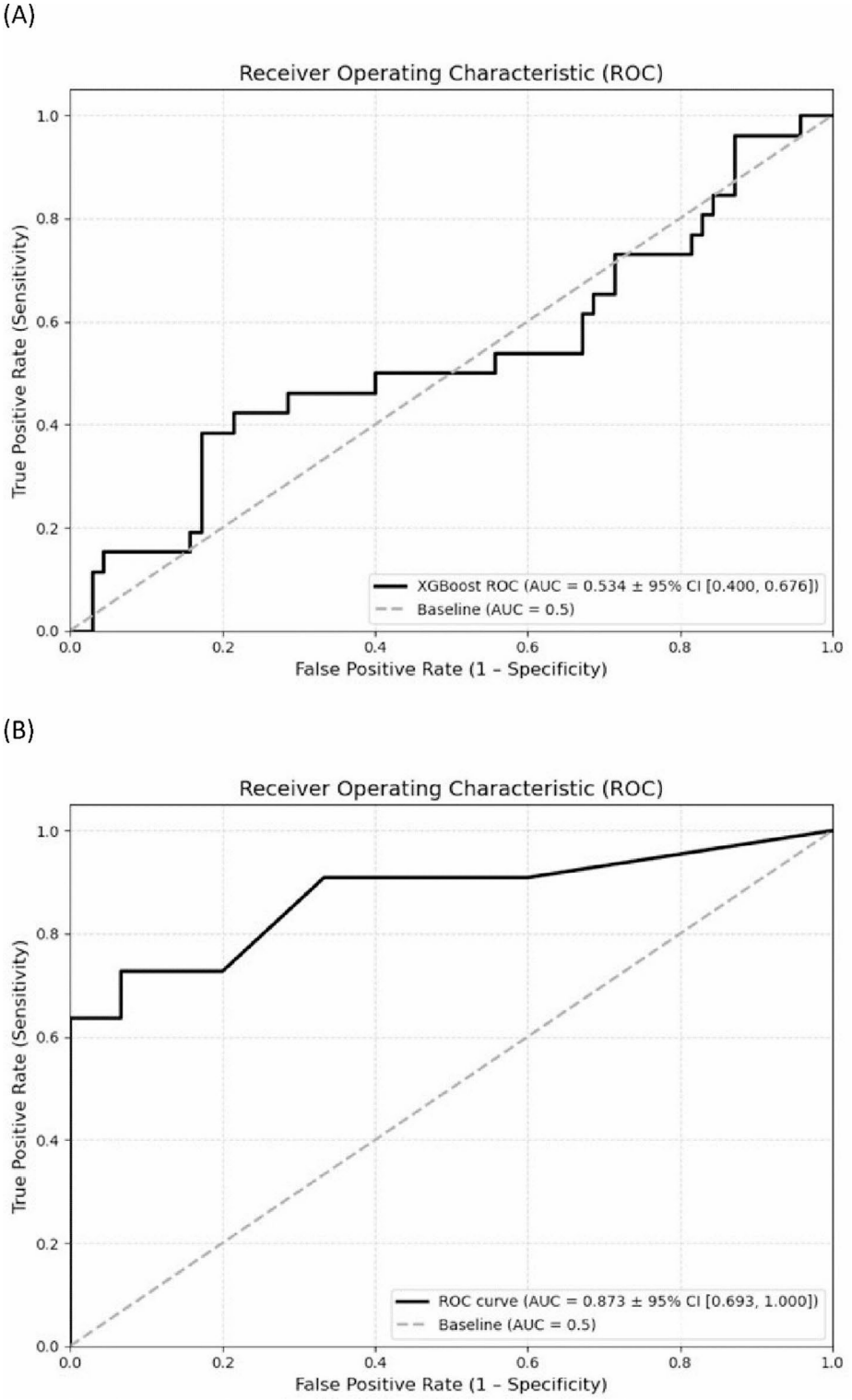


Fig. 2. ROC curve of final prediction model using XGBoost. (**A**) Stage 1, (**B**) Stage 4. The AUC of stage 1 is 53.4% and stage 4 is 87.3%, indicating better prediction of Stage 4 model.

Despite these constraints, our study possesses significant strengths. We have identified the most crucial sonographic variables that should be measured, which we believe can substantially contribute to improving the success rate of maturation. Addressing these factors has the potential to enhance the quality of life for dialysis patients, reduce healthcare costs, and minimize reintervention rates. Additionally, the data were collected from three different centers, each utilizing varying ultrasound machines, techniques, and surgical approaches. This diversity reflects the complexity of real-world clinical scenarios, enhancing the generalizability of our findings.

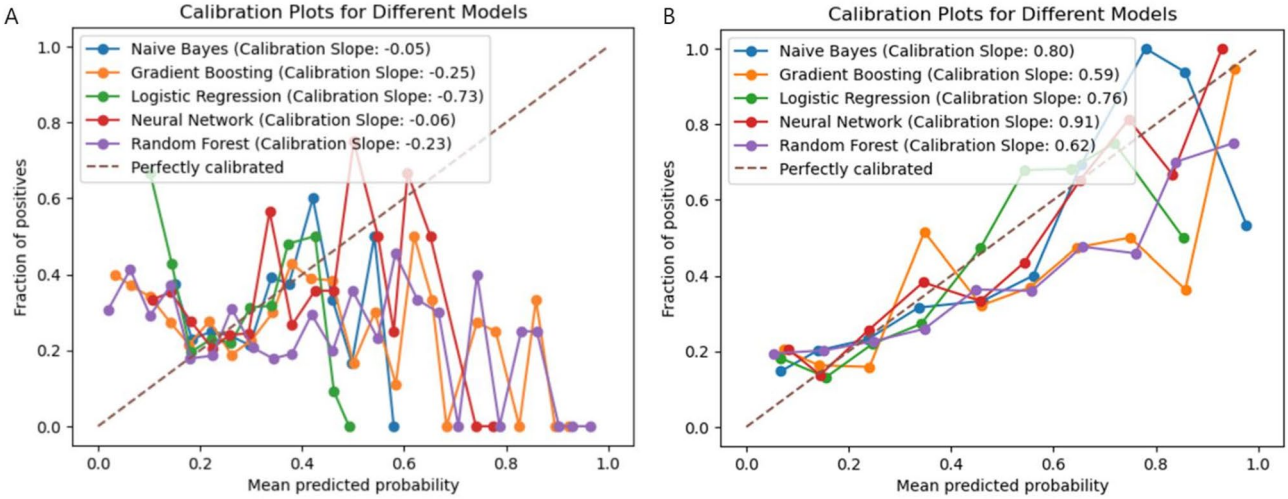


Fig. 3. Calibration plots for different models. (**A**) Stage 1, (**B**) Stage 4. Stage 4 model depicted better calibration plot than stage 1 model.

Model type	Dataset	Features used	Performance (AUROC/other metrics)	Comment	References
XGBoost Model (AVF Maturation Prediction)	Single/Multicenter Ultrasound	Ultrasound diameters, flow, clinical variables	AUROC approximately 0.79 to 0.81	Includes feature importance analysis; outperforms traditional clinical static criteria	20
Lasso & Elastic Net (AVF Prediction)	Mixed Forearm/ Upper Arm AVF cohorts	Peripheral vascular disease, vein diameter, sex	AUROC 0.68 (development), 0.59 (external validation)	Focus on clinical scoring; reasonable predictive performance	21
Deep Learning Models (Medical Imaging)	Various medical imaging datasets	Deep CNN, texture and morphological features	Varies by architecture; generally superior performance of deep models	Importance of network architecture optimization	[22]
Machine Learning vs. Deep Learning (Time Prediction/Generalization)	Time-series traffic data	Time-series features	XGBoost outperforms RNN-LSTM in MAE, MSE	In some data, ML outperforms DL in both interpretability and accuracy	[23]
Traditional Static Clinical Criteria (KDOQI, UAB)	Ultrasound and clinical data	Flow and diameter cutoffs	Lower net benefit compared to ML models	Easier clinical application but less flexible and accurate	20

Table 3. Comparison of the current model with recent state-of-the-art methods. AUC, area under the receiver operating characteristic curve; AVF, arteriovenous fistula; CNN, convolutional neural network; ML, machine learning; DL, deep learning; KDOQI, Kidney Disease Outcomes Quality Initiative.

Furthermore, a five-fold cross-validation approach was used to evaluate model performance. This method allowed for robust internal validation without splitting the dataset, given our limited sample size.

Nevertheless, further research is needed to suggest a cut-off value for measurement sites and to develop a model with improved predictive power, requiring an increased sample size or a prospective design. Moreover, while our model was internally validated using five-fold cross-validation across a multicenter dataset, external validation using independent cohorts from other institutions was not performed. This is primarily due to the current unavailability of appropriate external datasets with compatible preoperative ultrasound parameters. Future prospective multicenter studies incorporating external validation are warranted and are currently under planning through multi-institutional collaboration.

In conclusion, we achieved an AI-based prediction model using preoperative ultrasound data from the forearm cephalic vein at different sites. Unlike prior studies, we newly found that the identification of competing tributaries has been found to be crucial factors for successful radio-cephalic arteriovenous fistula maturation. This emphasizes the importance of tailored sonographic evaluation during preoperative ultrasound mapping, instead of solely focusing on the anastomotic site.

Methods

This retrospective cohort study used data to investigate the optimal prediction model for AVF maturation using AI modeling. The study followed the ethical principles of the Helsinki Declaration, and no patient was subjected to any new, alternative, or changed practices. The institutional ethics review board approved this cohort study and waived the need for informed consent due to the retrospective nature of the study (IRB No. S2020-3118-0001). The data was completely anonymized and used in machine learning or deep learning models. Imputation of missing values was not considered.

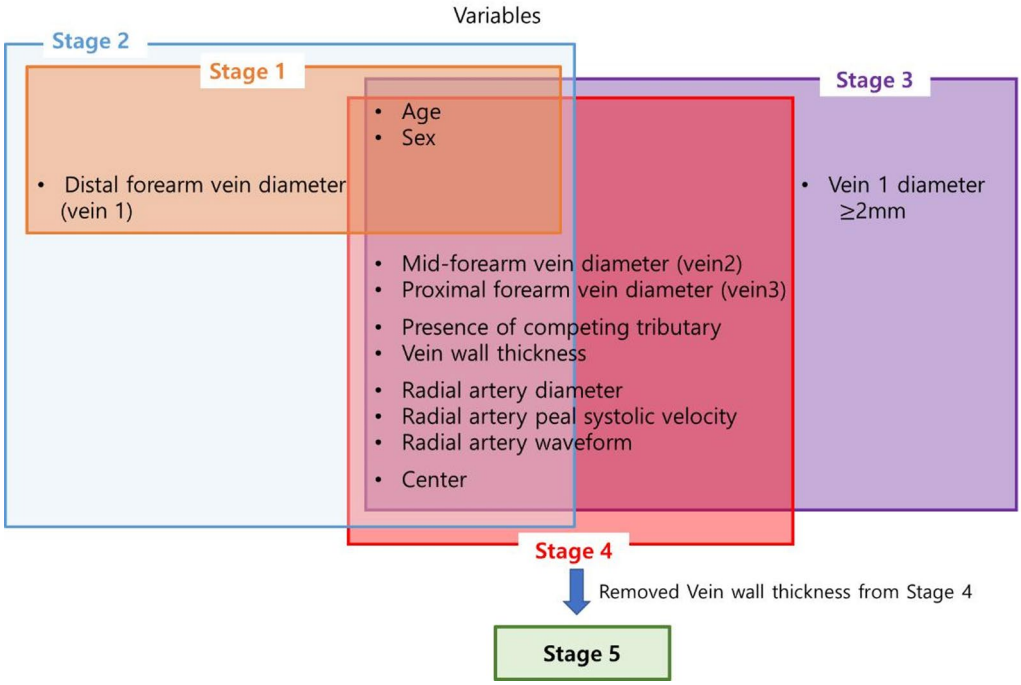


Fig. 4. Feature selection process. Stage 1 included age, sex, and vein 1 as variables. Stage 2 involved all collected variables. Stage 3 excluded vein 1 with a diameter less than 2 mm. Stage 4 included all variables except for vein 1. Stage 5 removed wall thickness from stage 4.

Study population

The study cohort included a total of 494 consecutive patients who underwent RC AVF due to advanced chronic kidney disease from 2018 to 2022 across three centers. Patients who did not have follow-up data available were excluded from the study.

Study outcome and feature selection

The outcome of the study was the maturation of the fistula. Fistula maturation was defined as an arteriovenous fistula that matures and is usable for dialysis with two-needle cannulation for hemodialysis for at least 90 days without endovascular or surgical interventions[4]. Demographic information such as age and sex, as well as anatomical variances including the diameter of the cephalic vein and radial artery, the waveform of the radial artery, the thickness of the cephalic vein, the presence of a large tributary of the cephalic vein, and the center, were taken into consideration. Anatomic data were obtained via preoperative duplex ultrasound mapping, which was performed on the same day as the scheduled surgical procedure across all three participating centers. The diameter (internal caliber) of the cephalic vein was measured at three points on the forearm: distal (vein 1), mid (vein 2), and proximal (vein 3), along its direct continuation to the median cubital fossa. Cephalic vein diameters were measured at three predetermined points: distal (1 cm from the wrist), mid (mid-forearm), and proximal (near the elbow). These standardized measurement points were used consistently across all cases. A competing tributary was defined as a venous side branch with a diameter comparable to that of the main cephalic vein outflow pathway. A fixed absolute diameter cutoff was not applied due to inter-individual variability in cephalic vein size; instead, a relative comparison to the main outflow vein was used. Tributaries that could be exposed through the surgical incision were routinely ligated and therefore excluded from this definition. Accordingly, competing tributaries were defined as those located outside the surgical exposure field, typically more than 3 cm from the planned anastomosis site. The thickness of the cephalic vein was measured at the anticipated anastomosis site. The diameter of the radial artery and its hemodynamic status, including peak systolic velocity (PSV) and waveform, were assessed. The arterial waveform was categorized as triphasic, biphasic, or monophasic. Certified vascular technicians with international licenses of vascular sonography performed all ultrasound examinations. A standardized protocol was followed across the three study centers to minimize inter-operator variability.

Feature selection process

The model was developed in five stages, each incorporating different variables (Fig. 4). In Stage 1, age, sex, and vein 1 were included as these variables are commonly considered in clinical practice. Stage 2 involved the inclusion of all collected variables. Moving on to Stage 3, vein 1 with a diameter less than 2 mm was excluded. Stage 4 included all variables except for vein 1. Finally, Stage 5 removed wall thickness from Stage 4 while retaining all other variables in the final model. Factors were selected based on clinical relevance and statistical

correlation with maturation success in prior studies. Each model stage was designed to evaluate the added predictive value of specific variables.

Statistical methods

When reporting descriptive statistics, categorical variables were summarized using frequencies and percentages. For continuous variables that followed a normal distribution, the mean and standard deviation were reported. In cases where the distribution deviated from normality, the median and interquartile range were utilized instead. Before implementing machine learning techniques, the $\chi 2$ test was conducted for categorical variables, while the Mann-Whitney U test was used for continuous variables. A significance level of $p < 0.05$ was employed to determine statistical significance.

To create a highly effective predictive classification model, we explored several modeling procedures, including Gradient Boosting (XGBoost), Naïve Bayes, random forest, and neural network. For the machine learning analysis, an extreme gradient boosting (XGBoost) model was implemented with the following hyperparameters: learning rate of 0.3, maximum tree depth of 6, and 10 estimators. Subsampling was applied when appropriate to improve generalizability. A neural network model was also constructed with a single hidden layer consisting of 20 neurons. The model was trained using the Adam optimizer with a learning rate of 0.001. Feature importance was assessed using permutation importance, which evaluates the decrease in model performance when individual features are randomly permuted, thereby reflecting their contribution to prediction accuracy. For classification problems, the standard approach was multilinear logistic regression. All of these predictive modeling methods followed a training, hyperparameter tuning, and testing process. As mentioned earlier, the input features consisted of baseline clinical characteristics and preoperative ultrasound parameters. Before fitting the models, continuous variables were standardized by scaling their distributions (dividing by the standard deviation). We built the models using the entire dataset and tuned the hyperparameters using grid search methods with nested 5-fold cross-validation. After hyperparameter tuning, the final models were re-fit on the complete training dataset. The primary performance indices we used were the F1 score, Matthews Correlation Coefficient (MCC), precision, and recall. The F1 score was particularly suitable for imbalanced class metrics as it considers both sensitivity and specificity. The Matthew's Correlation Coefficient (MCC) is a metric that assesses predictive power by considering both classes. It remains stable even with imbalanced datasets. The values of MCC range from −1 to 1, where values closer to 1 indicate perfect predictions, 0 represents random predictions, and −1 represents completely incorrect predictions. Typically, a value above 0.5 suggests good classification performance. The performance of the final model was evaluated using a hold-out testing dataset. A classification threshold of 0.5 was applied to all models. Receiver Operating Characteristic (ROC) curves, calibration plots, and decision curve plots were generated for each modeling approach. Performance metrics such as the area under the ROC curve (AUROC), sensitivity, specificity, accuracy, and logistic calibration slope and intercept were calculated for each modeling approach. The calibration slope was compared between models with the best and worst performance. If the calibration slope is greater than 1, the model tends to overestimate predictions. If the calibration slope is less than 1, the model tends to underestimate predictions.

Data availability

The datasets generated during and/or analyzed during the current study are available from the corresponding author on reasonable requests.

Received: 9 November 2025; Accepted: 16 April 2026
Published online: 21 April 2026

References

1. Perera, G. B. et al. Superiority of autogenous arteriovenous hemodialysis access: Maintenance of function with fewer secondary interventions. *Ann. Vasc. Surg.* **18**, 66–73 (2004).
2. Vascular Access Work, G. Clinical practice guidelines for vascular access. *Am. J. Kidney Dis.* **48**, S248–S273 (2006).
3. Georgiadis, G. S., Charalampidis, D. G., Argyriou, C., Georgakarakos, E. I. & Lazarides, M. K. The necessity for routine pre-operative ultrasound mapping before arteriovenous fistula creation: A meta-analysis. *Eur. J. Vasc. Endovasc. Surg.* **49**, 600–605 (2015).
4. Lok, C. E. et al. KDOQI clinical practice guideline for vascular access: 2019 update. *Am. J. Kidney Dis.* **75**, S1–S164 (2020).
5. MacRae, C., Mercer, S. W., Guthrie, B. & Henderson, D. Comorbidity in chronic kidney disease: A large cross-sectional study of prevalence in Scottish primary care. *Br. J. Gen. Pract.* **71**, e243–e249 (2021).
6. Tummalapalli, S. L., Chu, C. D. & Tuot, D. S. Avoiding overuse of venipuncture and laboratory testing in hospitalized patients on hemodialysis. *J. Patient Saf.* **18**, e225–e226 (2022).
7. Dageforde, L. A., Harms, K. A., Feurer, I. D. & Shaffer, D. Increased minimum vein diameter on preoperative mapping with duplex ultrasound is associated with arteriovenous fistula maturation and secondary patency. *J. Vasc. Surg.* **61**, 170–176 (2015).
8. Zamboli, P., Punzi, M., Bracale, U. M. & Pisani, A. Early predictors of arteriovenous fistula maturation: Preoperative arterial diameter alone is not enough. *J. Am. Soc. Nephrol.* **31**, 2226–2228 (2020).
9. Lauvao, L. S. et al. Vein diameter is the major predictor of fistula maturation. *J. Vasc. Surg.* **49**, 1499–1504 (2009).
10. Chlorogiannis, D. D. et al. Pre-operative ultrasound mapping before arteriovenous fistula formation: an updated systematic review and meta-analysis. *J. Nephrol.* **37**, 281–292 (2024).
11. Vo, A. T. T. et al. Revisiting the role of ultrasound mapping in arteriovenous fistula formation: a single-center experience. *J. Vasc Ultrasound.* **46**, 160–164 (2022).
12. Thomas, B. et al. Maintenance dialysis throughout the world in years 1990 and 2010. *J. Am. Soc. Nephrol.* **26**, 2621–2633 (2015).
13. Hakim, A. J., Brooke, B. S., Beckstrom, J. L., Sarfati, M. R. & Kraiss, L. W. Rules of 6 criteria predict dialysis fistula maturation but not all rules are equal. *J. Vasc. Surg.* **76**, 232-238.e2 (2022).
14. Zangan, S. M. & Falk, A. Optimizing arteriovenous fistula maturation. *Semin. Intervent. Radiol.* **26**, 144–150 (2009).
15. Robbin, M. L. et al. Hemodialysis arteriovenous fistula maturity: US evaluation. *Radiology* **225**, 59–64 (2002).

16. Hou, G. et al. Preoperative cephalic vein diameter and diabetes do not limit the choice of wrist radio-cephalic arteriovenous fistula. *J. Vasc. Access* **21**, 366–371 (2020).
17. Troupes, C., Png, C. Y. M., Bhattarai, P. & Finlay, D. J. Small caliber distal cephalic veins undergo significant dilation under anesthesia and can successfully be used for arteriovenous fistula creation. *Ann. Vasc. Surg.* **96**, 316–321 (2023).
18. Heindel, P. et al. Predicting radiocephalic arteriovenous fistula success with machine learning. *npj Digit. Med.* **5**, 160 (2022).
19. Siddiqui, M. A. et al. Predictive parameters of arteriovenous fistula maturation in patients with end-stage renal disease. *Kidney Res. Clin. Pract.* **37**, 277–286 (2018).
20. Zhou, S. K. et al. A review of deep learning in medical imaging: Imaging traits, technology trends, case studies with progress highlights, and future promises. *Proc. IEEE* **109**, 820–838 (2021).
21. Santoro, D., Ciano, T. & Ferrara, M. A comparison between machine and deep learning models on high stationarity data. *Sci. Rep.* **14**, 19409 (2024).

Author contributions

S.A. and A.C. equally contributed to this work as first authors. Conceptualization, S.A. and H.K.; Data Curation, S.A., A.C., J.K., and H.K.; Formal analysis, J.H. and Y.K.; Funding acquisition, H.K.; Methodology, S.A. and H.K.; Writing-original draft, S.A., A.C., and H.K.; Writing- review & editing, S.A. A.C., J.K., and H.K.; Visualization, J.H. and Y.K.

Funding

This study was supported by the Lee Yong Gak Research fund of the Korean Society for Vascular Surgery and a general research grant from Seoul National University Hospital (No. 800-20210425).

Declarations

Competing interests

The authors declare no competing interests.

Additional information

Correspondence and requests for materials should be addressed to H.K.

Reprints and permissions information is available at www.nature.com/reprints.

Publisher's note Springer Nature remains neutral with regard to jurisdictional claims in published maps and institutional affiliations.

Open Access This article is licensed under a Creative Commons Attribution-NonCommercial-NoDerivatives 4.0 International License, which permits any non-commercial use, sharing, distribution and reproduction in any medium or format, as long as you give appropriate credit to the original author(s) and the source, provide a link to the Creative Commons licence, and indicate if you modified the licensed material. You do not have permission under this licence to share adapted material derived from this article or parts of it. The images or other third party material in this article are included in the article's Creative Commons licence, unless indicated otherwise in a credit line to the material. If material is not included in the article's Creative Commons licence and your intended use is not permitted by statutory regulation or exceeds the permitted use, you will need to obtain permission directly from the copyright holder. To view a copy of this licence, visit http://creativecommons.org/licenses/by-nc-nd/4.0/.

© The Author(s) 2026